USE OF DIFFERENT SHAPED STEEL SLIT DAMPERS IN BEAM TO COLUMN CONNECTIONS OF STEEL FRAMES UNDER CYCLING LOADING

Mehmet Alpaslan Köroğlu[1,*], Ali Köken[2] and Yunus Dere[1]

[1] *Dept. of Civil Engineering, Necmettin Erbakan Univ., Konya 42060, Turkey*
[2] *Dept. of Civil Engineering, Selcuk Univ., Konya 42075, Turkey*
**(Corresponding author: E-mail: makoroglu@konya.edu.tr)*

Received: 21 August 2017; Revised: 29 September 2017; Accepted: 1 November 2017

ABSTRACT: Following the Northridge and Kobe earthquakes, extensive research was conducted on the use of various materials and systems that will absorb the earthquake effects within the structure itself in order to improve the behavior of the steel structures under seismic effects. In this study, the use of seismic dampers at beam-column joints of steel-framed structures to prevent damage to the structural members by absorbing the energy of the lateral loads was investigated. Thus, it will be possible for the steel-framed structures to be put into service right after a damaging earthquake by only replacing the dampers attached to the joints as no damage will occur to the beams and columns. For this purpose, as a first step, dampers with ductile behavior were chosen through preliminary tests. Consistent with the results of the preliminary tests, a total of six full-scale corner beam-column joint test specimens were produced. Five specimens were attached various types of dampers in different sizes and one reference specimen was designed with regular end-plate connection.

After the evaluation of the test results, valuable data on the load carrying and energy consumption capacities, stiffness characteristics and the general behavior of the specimens were obtained. In the analytical part of the study, analyses of the selected specimens were performed through ANSYS finite elements software package. The analytical and experimental results were compared and have been found very consistent with each other.

Keywords: Beam-column joint, steel slit damper, steel frame, seismic damper, finite element

DOI: 10.18057/IJASC.2018.4.2.7

1. INTRODUCTION

Structures built throughout history were damaged by the earthquakes that caused devastating property damage and loss of lives. Therefore, different solutions to minimize the destructive effects of earthquakes were proposed with the impact of technological advances of the last century. Structural control mechanisms based on the principle of damping the seismic energy through non-structural members were developed. Among these members, metallic dampers are economical, easy-to-produce, and can effectively dissipate seismic energy through hysteretic behavior. The use of metallic dampers attracted the attention of researchers, especially after the unexpected damages to the joints of the steel framed structures in the Northridge (1994) and Kobe (1995) earthquakes [1] Many types of metallic dampers have been developed so far. The most popular among these are stiff dampers which are called ADAS (Added Damping and Stiffness) [2]. These members are made of high ductility steel and usually attached to steel frames. When built in triangular shape and produced from mild steel, they are called TADAS (Triangular Added Damping and Stiffness) [3]. They are welded at the bottom and bolted at the top and attached to the beam-column joints. In addition to these, honeycomb dampers [4], buckling restrained braces [5], bell shaped metallic dampers, lead-added metallic dampers and pi dampers are also available [6]. Passive energy steel dampers which are created by opening holes on steel plates are called slit dampers [7]. Recently, these metallic dampers have become increasingly popular. Especially following the Northridge (1994) and Kobe

(1995) earthquakes, the use of passive energy dampers at different regions of steel structures became quite common. A variety of dampers in different shapes and sizes were used for this purpose.
Oh et al. [1], used slit dampers at steel beam-column joints for the first time in the literature. Performing four full scale beam-column joint experiments, the researchers managed to dissipate the energy of the applied cyclic loads without causing any damage to the columns and beams. They investigated the behavior of the steel dampers of different geometric shapes in IPE type steel beams under cyclic loadings, different from other researchers.

Steel slit dampers were used by many researchers in moment resisting frames and in the center of X bracings (Lee et al., [7], Chan and Albermani [8]). And slit dampers have been used at beam-column joints recently [1, 9-14].

In this study, the use of dampers attached to the beam-column joint of a moment resisting frame that provides resistance to earthquakes preventing damage to the column or beam by damping the effects of lateral loads was investigated. Dampers are welded plates having bolt holes at their top and bottom edges for easy installation. They are attached to the beam-column joint by bolting both to the bottom flange of the beam and to the gusset plate (lower split-T) of the column. Therefore, they can be easily replaced when they get damaged during an extensive earthquake. The slit dampers with lower split-T can also be replaced easily [1]. However, in this study, changing only the damper will be sufficient. Moreover, one damper was used for narrow flanged beams as opposed to using two dampers as in [1].

A two stage experimental research was conducted for the use of dampers at beam-column joints. First, preliminary tests were performed in order to determine the appropriate type of damper. Thus, nine dampers with different geometric shapes previously used at different locations of steel frames in the literature were considered and experimentally evaluated. In line with the test results, three types of dampers were selected to be used in the full scale steel beam-column joint tests which constitute the core of this study. The behavior of dampers with different geometric shapes was compared with each other and the experiments were modeled using finite element method.

2. MATERIAL AND METHOD

In this study, the use of dampers at beam-column joints of steel frames was investigated. The experimental part of the study was composed of two stages. In the first stage, a test system to apply shear force to the dampers was developed in order to investigate the behavior of the dampers having nine different geometric shapes subjected to cyclic loading. These experiments were referred to as preliminary tests in this study. In the second stage, based on the preliminary test results, the feasible damper types were determined. Afterwards, an experimental system for the tests of the full scale beam-column joints was created. The full scale tests were performed in order to investigate the use of dampers at beam-column joints.

3. TEST SPECIMENS USED IN THE PRELIMINARY TESTS AND THEIR PROPERTIES

In this section, the geometric shapes of the produced dampers were determined based on the dampers from the literature that were used at different locations of steel structures. In the preliminary tests, damper shapes were chosen based on the ones available in the literature that are located either at the joints where x-bracings meet the column and beams or at the foundation joints of columns. The dampers with the most suitable geometry for the full-scale beam-column joint tests were selected regardless of their load bearing capacities. A rigid loading frame that can apply reversed-cyclic loads was developed as the testing apparatus of the preliminary tests.

One edge of the damper was fixed to one of the columns of the rigid frame by bolts whereas the other edge of the damper was bolted to the connector plate attached to the load cell and the hydraulic pump that can apply reversed-cyclic loading. (Figure 1).

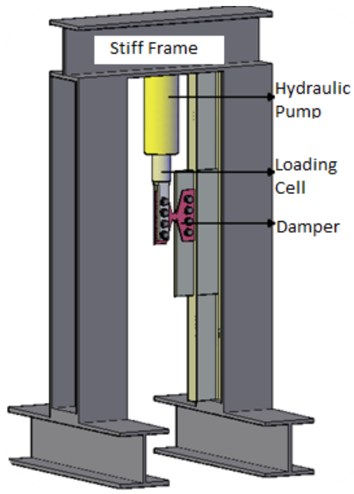

Figure 1. Test Apparatus used in the Preliminary Tests

Three steel specimens made of St-37 type steel material and complying with the European standards were tested. The results obtained from the tensile tests are listed in Table 1. In Figure 2, various types of dampers considered during the preliminary tests are presented. At the end of the tests, considering the ductility, loading bearing capacity and stability of these geometric shapes, the decision was made for the use of three dampers displayed in Figure 3 which are called slit, L-shaped and round-hole type dampers.

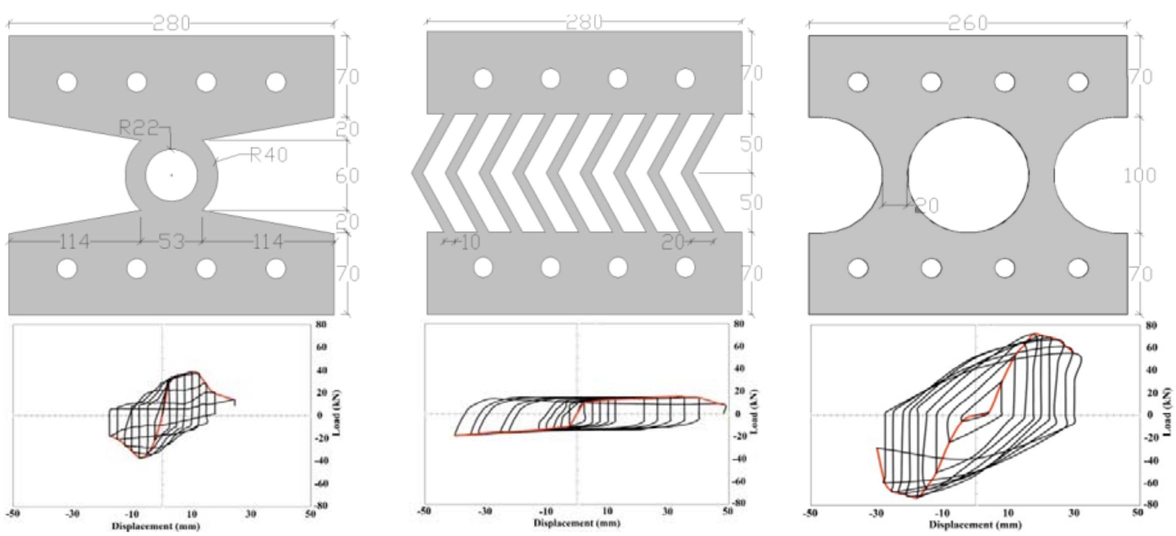

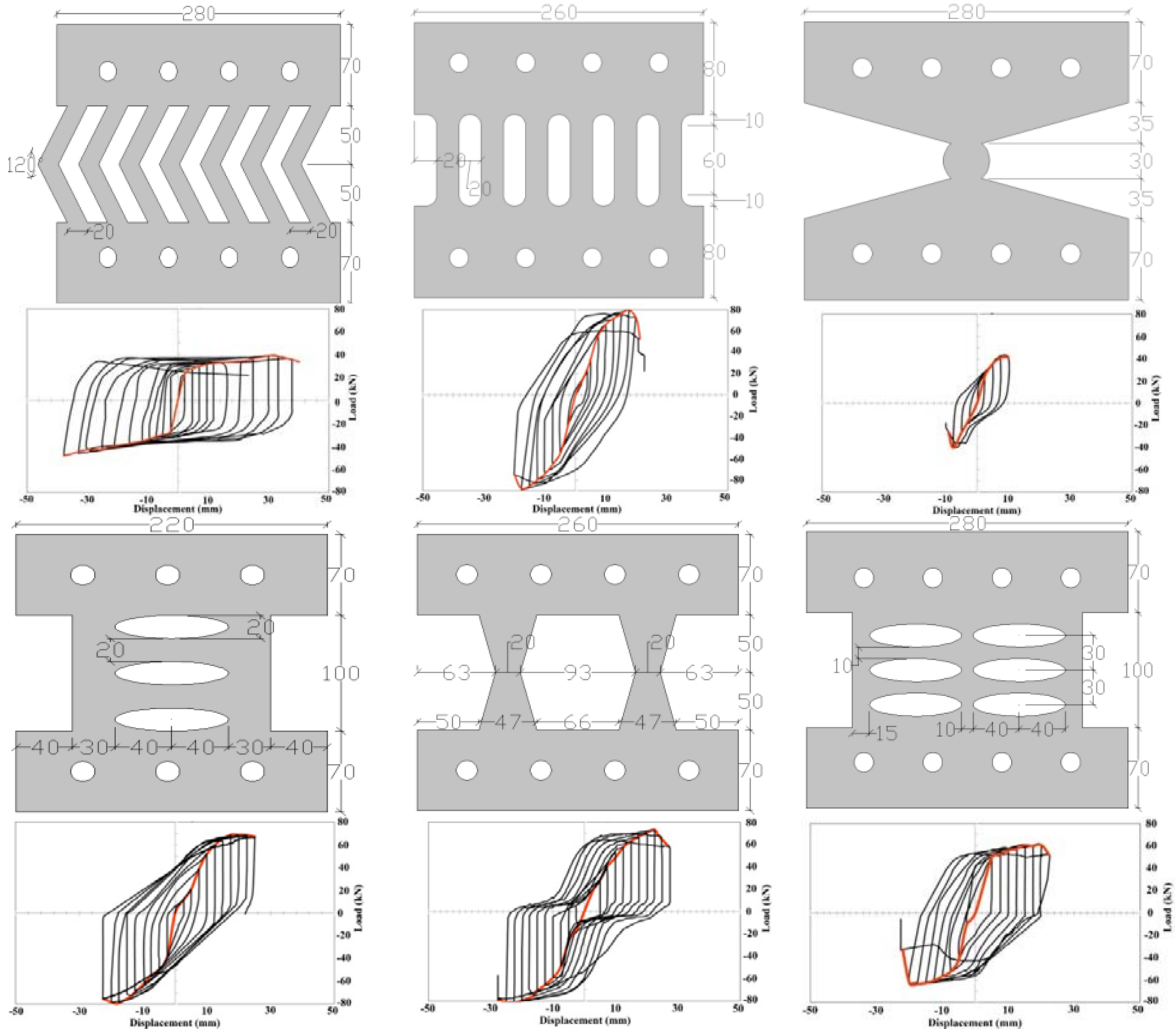

Figure 2. Various Types of Dampers Considered during the Preliminary Tests (Koroglu 2011,2012)

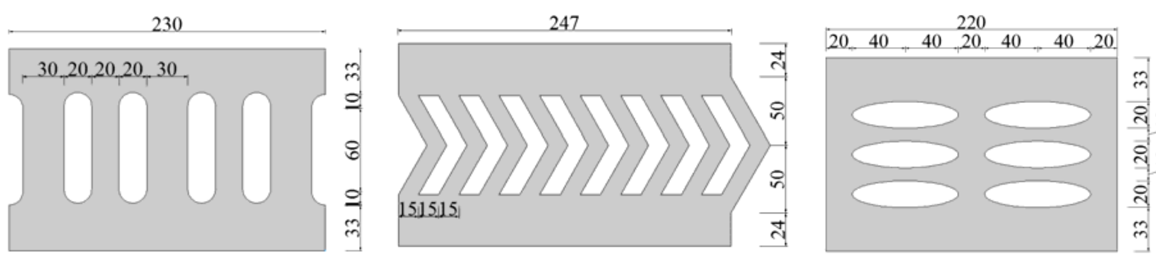

slit damper L-shaped round hole

Figure 3. Damper Types Determined after the Preliminary Tests

Table 1. Tensile Test Results of Steel Material used in the Preliminary Tests

Test No	**Width** (mm)	**Thickness** (mm)	**Elasticity Module** (MPa)	**Yielding Stress** (MPa)	**Max Stress** (MPa)	**Failure Stress** (MPa)	**Failure Strain** (%)
1	24.90	10.00	210,6	302.40	414.60	312.40	33.20
2	25.10	10.05	209,9	301.70	411.40	321.30	34.60
3	24.90	10.00	209,4	303.40	421.30	304.80	35.10
		Average	209976	302.50	415.77	312.83	34.30

4. FULL SCALE TESTS OF THE BEAM-COLUMN JOINTS OF STEEL FRAMES

In the literature, there are two different test configurations available for the full scale beam-column joint tests. These test configurations are different for the corner and middle columns.

In this study, the test configuration for the corner columns is selected for the full scale tests. Test specimens were pin-supported at the zero moment points, i.e. at the center points of the upper and lower floor columns in order to reflect the real frame behavior. The beam at floor level was subjected to reversed-cyclic loading right at the center point (Figure 4).

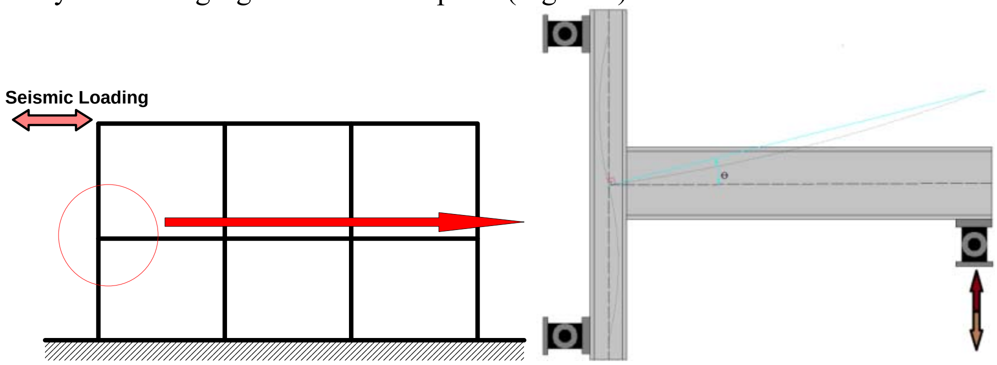

Figure 4. Idealization of the Beam-column Joint.

The target with this damper-attached connection system was to absorb the energy during a severe earthquake by having the steel slit damper damaged without causing any damage to the column or beam. Afterwards, the damaged steel slit damper can be rapidly and easily replaced so that the structure could be put back into service safely. For this purpose, in this joint configuration, a plate is welded at the top and bottom edges of the slit damper. One plate is bolted to the beam's lower flange by high strength bolts, and the other to a rigid split-T gusset plate attached to the column. To constitute the beam support allowing rotations, the beam's upper flange is bolted to a split-T member attached to the column (Figure 5).

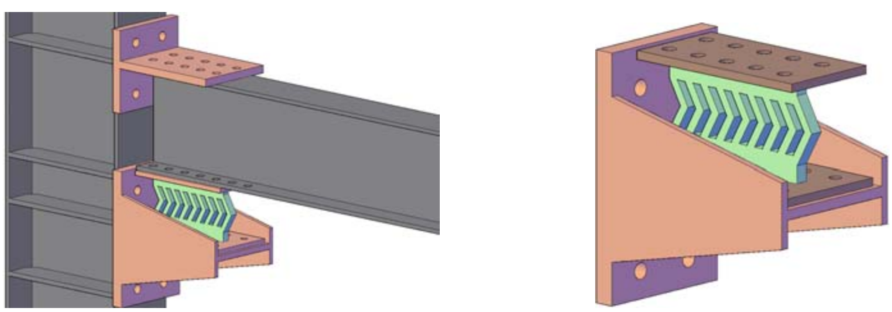

Figure 5. The Details of Beam-column Joint Utilizing a Slit Damper.

Unlike in the study by Oh et al. [1], in order to ease the use of narrow flange beams and also to allow damper edges to be welded at both sides, single damper was used instead of two. The welded plates will allow easy installation and replacing of damper.

5. TEST PROGRAM

Six full scale beam-column joint tests were carried out in an adaptive manner. First, a specimen with rigid end-plate connection was created as a reference. Then, a 12 mm thick steel slit damper (12D) without reinforcing the beam and a 15 mm thick steel slit damper (15D) with beam stiffeners were tested. Later, a 22 mm thick L-shaped steel damper (22E) was tested without reinforcing the beam. This damper was found to be weak at one direction and therefore a 15 mm thick double-skewed L-shaped (15E) damper was designed and tested (Figure 6.c). Finally, a 15 mm thick round holed damper was tested (15Y).

5.1 Test Specimens

In the full scale experiments, IPE 400 and IPE 270 type sections were chosen for columns and beams, respectively. The height of the column measured from the lower hinge to the upper hinge was 3m. The beam length measured from the point of load application up to the column's face was 2m. In the full scale tests, the damper-attached beam-column joint was detailed a little differently from the commonly used end plate connection. A "T- plate" connecting the beam to the column from the upper beam flange was manufactured by cutting a HEA 600 type profile while the gusset that transfers forces from the lower flange of the beam to the columns through the damper was manufactured from HEA 800 type profile. The gusset was stiffened with members welded at the top and bottom corners. Two types of steel material namely, St-37 and St-44, were used in the full scale tests. The material of IPE 270 and IPE 400 type profiles, the gusset and the upper T-plate was of St-44 standard. On the other hand, St-37 type material was used for the continuity plate, the end plate and the dampers. Joint details of the test specimens are presented in Figure 6. The mechanical properties of the materials obtained from the tension tests are provided in Table 2.

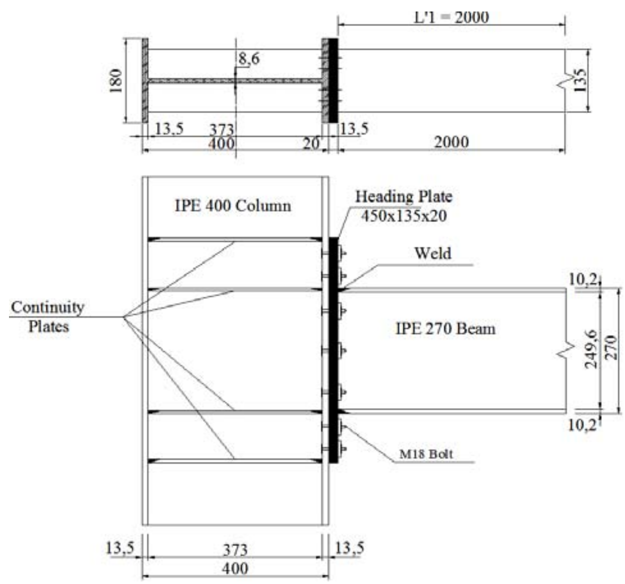

(a) Connection detail with end plate

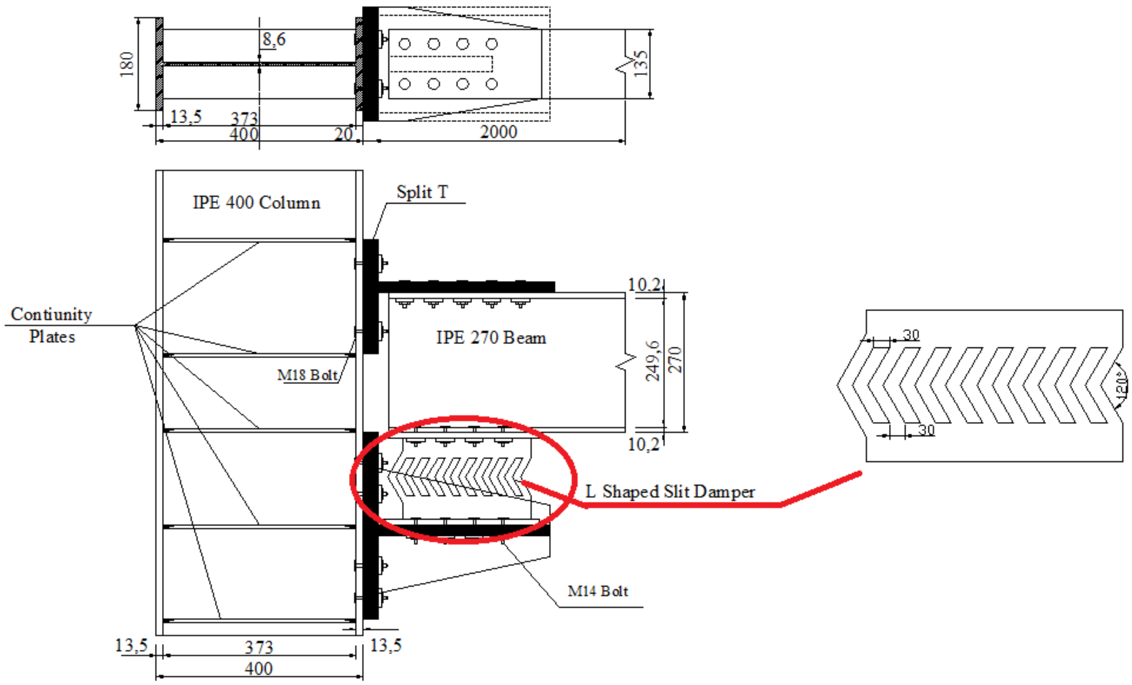

(b) Connection detail with damper

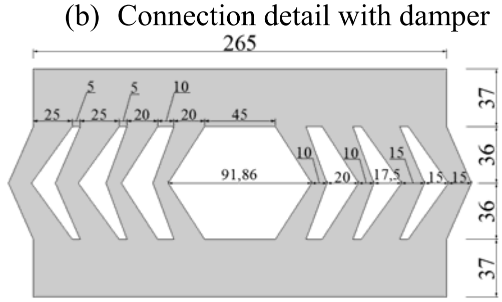

c) Geometric details of 15E damper

Figure 6. Joint Details of the Test Specimens

Table 2. Mechanical Properties of the Steel

Test Specimen		Steel grade	σ_y (MPa)	σ_u (MPa)	Ɛ (%)
Beam		St-44	319.40	458.22	27.4
Column		St-44	308.40	443.50	29.4
Split T	Gusset	St-44	322.40	457.45	26.3
	Upper T	St-44	329.35	465.10	25.9
Damper	(t=22 mm)	St-37	314.00	407.00	33
	(t=12 mm)	St-37	314.10	402.20	31
	(t=15 mm)	St-37	315.20	403.00	32

Welded and bolted connections were both utilized in the test specimens. All bolts were of high strength type bolts with a minimum failure stress of 800 MPa and a minimum yield strength of 640 MPa. The type of welding applied at the test specimens was gas metal arc welding and only fillet welds were performed. The diameter of the bolts and the thickness of welds were at their maximum allowed values so that no damage would occur in these members. Thus, no damage was detected at the welds and bolts during the tests.

Displacements were checked in all the tests carried out. Load control was enforced based on the load cycles presented in the study by Pachoumis et al. [15], which complies with FEMA-351 [16] and the regarding values are provided in Figure 7.

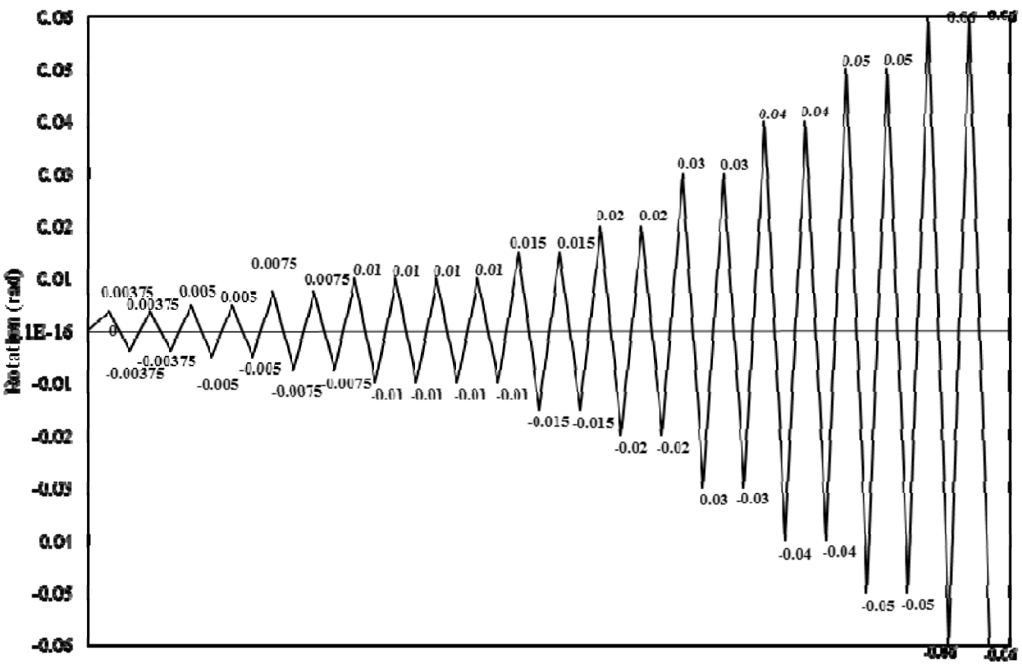

Figure 7. The load pattern applied during the tests

6. RESULTS OF THE RESEARCH

The full scale tests of six beam-column joint specimens, two with slit dampers, two with L-shaped dampers, one with round hole dampers and one with regular extended end plate, were performed. From the specimens with slit dampers, one specimen with a 12 mm thick slit damper was connected to the unreinforced beam, while the other specimen with a 15 mm thick damper was connected to the beam reinforced with two stiffeners. From the specimens with L-shaped damper, the specimen with 22 mm thick damper was connected to the unreinforced beam, whereas the other with 15 mm thick damper was connected to the beam reinforced with two stiffeners. On the other hand, 15 mm thick round-hole damper was connected to the beam reinforced with two stiffeners. The model drawings of test specimens can be seen in Figure 8.

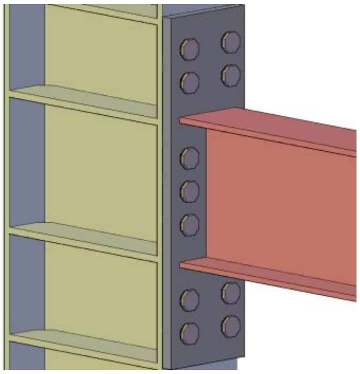

Extended End Plate (Reference)

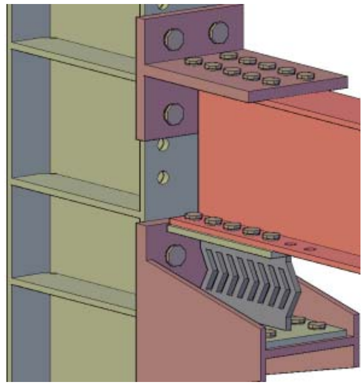

22E specimen

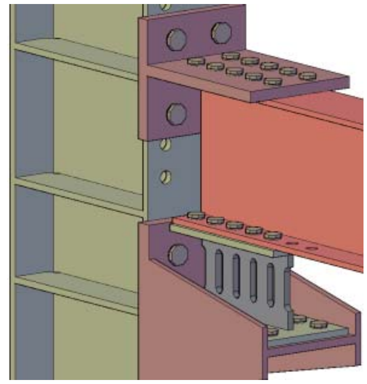

12D specimen

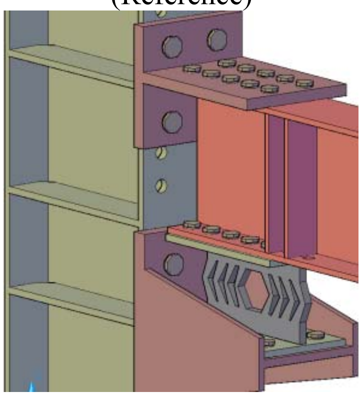

15E specimen

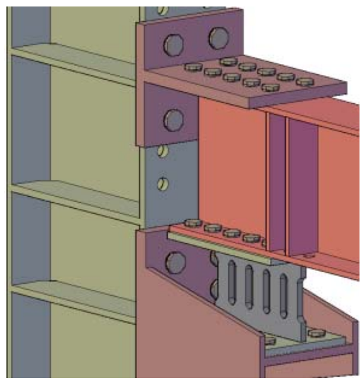

15D specimen

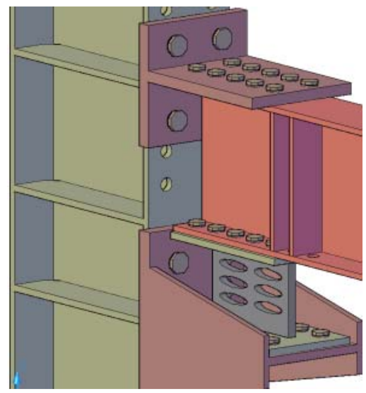

15Y specimen

Figure 8. Test Specimens

The purpose of the experiment with the unreinforced beam under cycling loading was to concentrate the damage on the damper by preventing any damage to the beam, before reaching the beam’s theoretical moment capacity i.e. staying within the elastic range. On the other hand, the aim with the reinforced beam specimen was to dissipate the energy by damaging the damper and having no damage on the beam although the theoretical moment capacity of the beam would be exceeded. The theoretical yield moment for the IPE 270 section was calculated as 132.8 kNm. This limit value was marked on the moment-rotation graph with dashed lines in Figure 9-14.

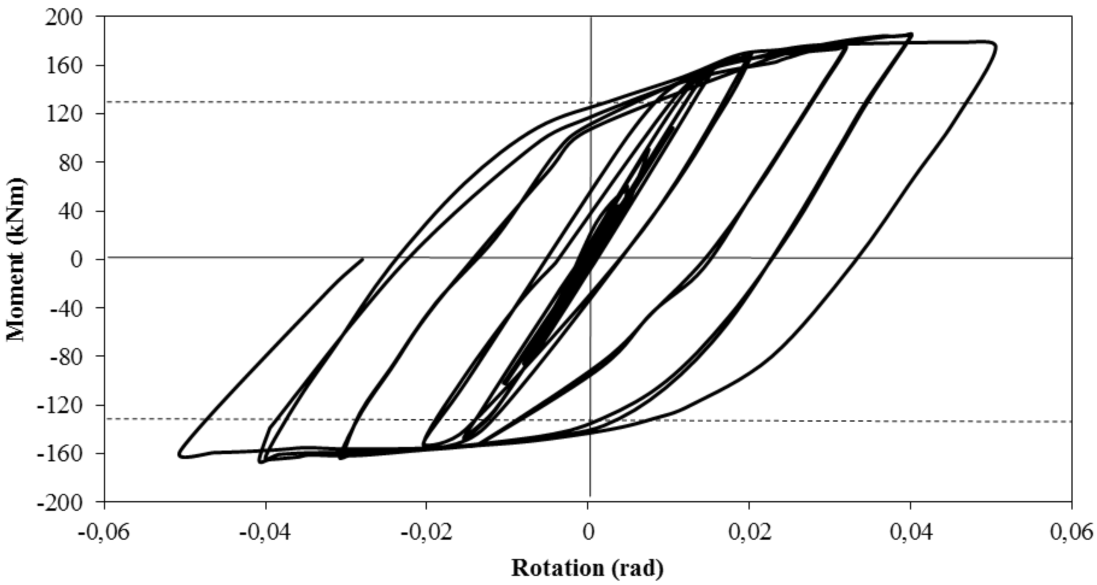

Figure 9. Moment-Rotation Diagram of the Reference Specimen

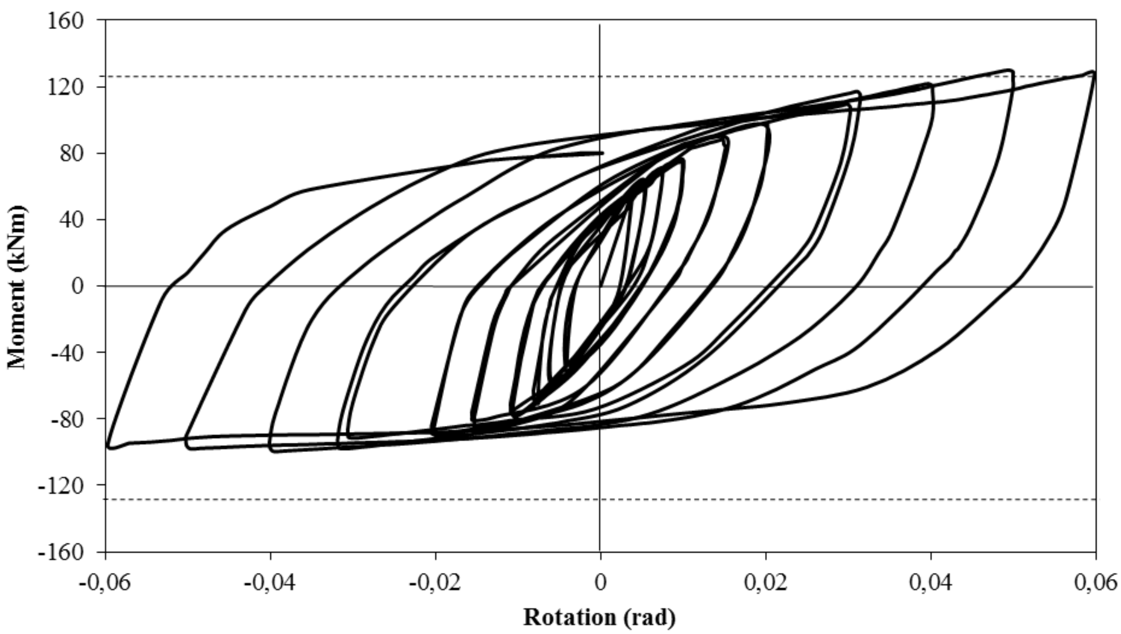

Figure 10. Moment-Rotation Diagram of Specimen 22E

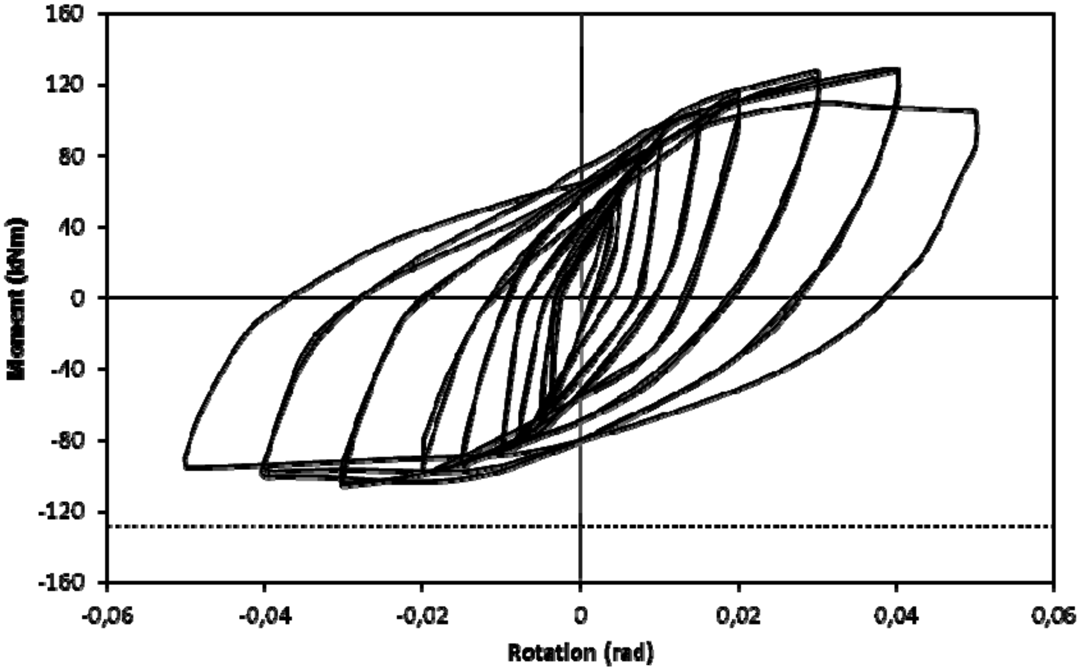

Figure 11. Moment-Rotation Diagram of Specimen 12D

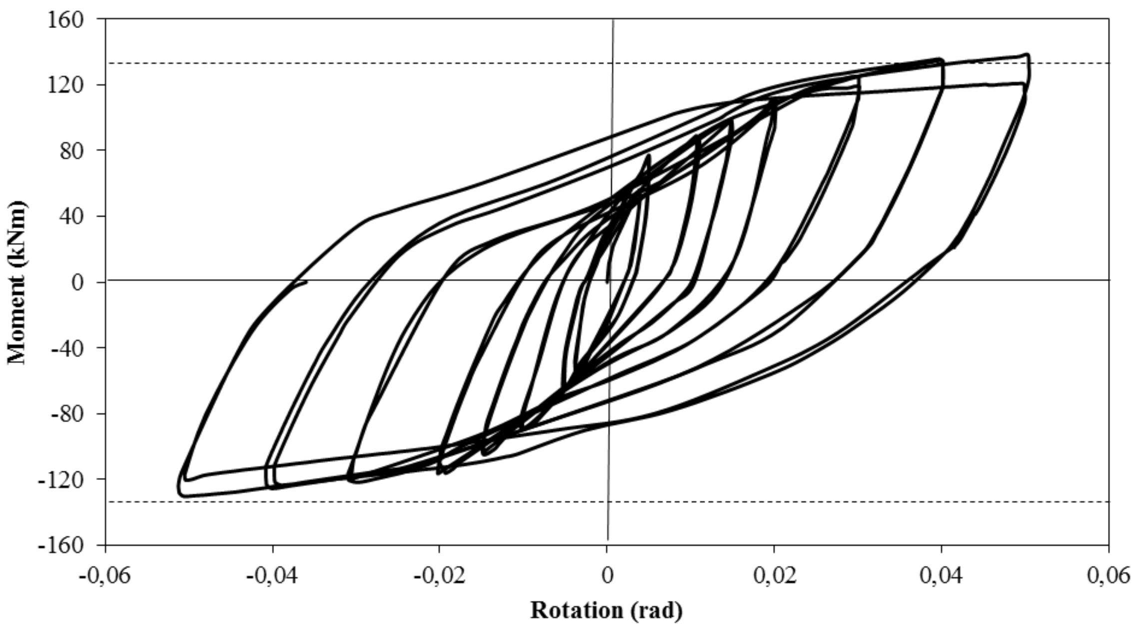

Figure 12. Moment-Rotation Diagram of Specimen 15E

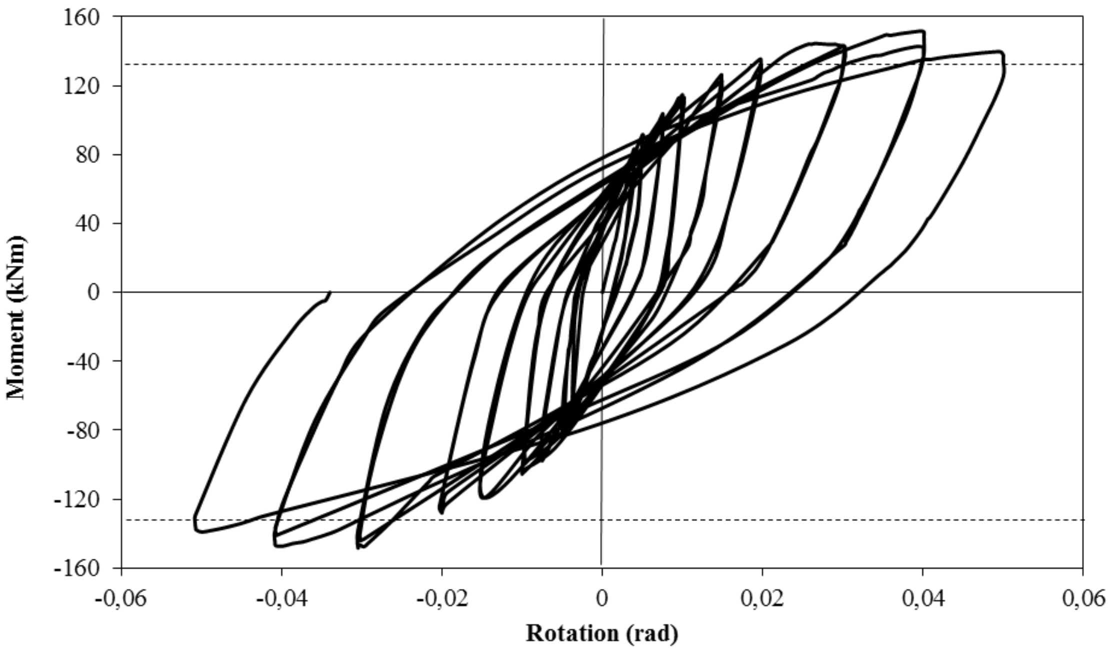

Figure 13. Moment-Rotation Diagram of Specimen 15D

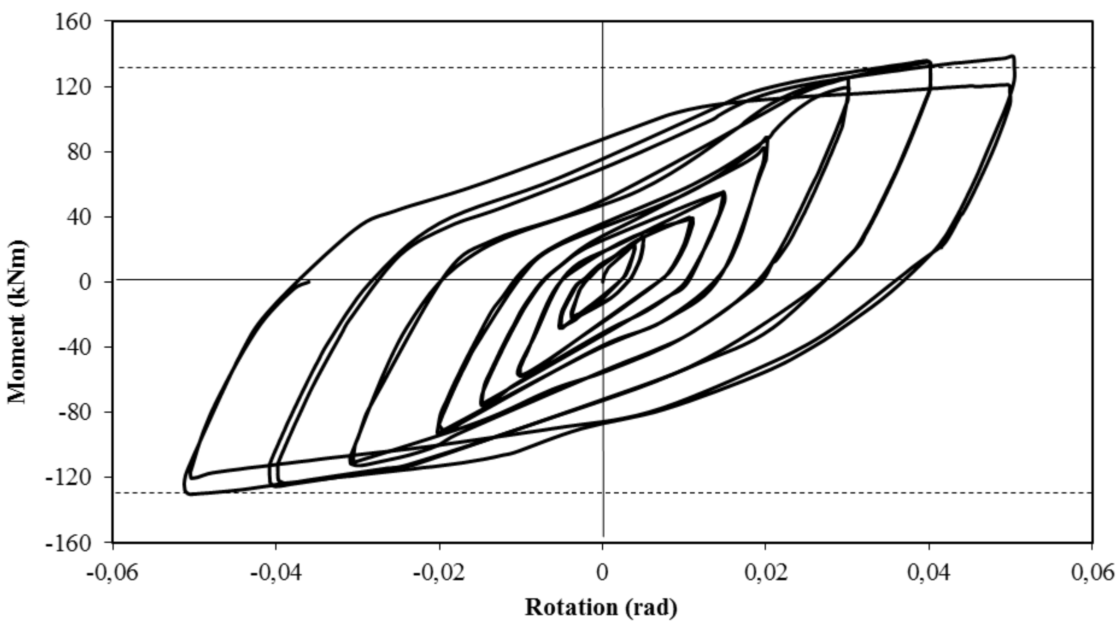

Figure 14. Moment-Rotation Diagram of Specimen 15Y

No permanent damage was observed during loading in any of the test specimens until a rotation value of 0.02 radians. After this rotation value, local buckling started to occur in the lower flange of the specimen with the extended end plate. Moreover, the plastic deformations in the test specimens with dampers occurred only on the dampers with no sign of damage on the beams. In further load steps, particularly above 0.02 radians of rotation, the local buckling of the lower flange of the beam was obvious in the reference specimen and excessive deformations and damage occurred at the dampers of the test specimens (Figure 15). Some cracks were observed at the upper part of the damper's end stud at 0.04 radians rotation in the specimen 12D. For the specimen 15D with thicker stud, the cracks at the damper occurred at 0.06 radians rotation. The deformation was apparent at 0.02 radians rotation and micro cracks were detected at the elliptical ends in the specimen 15Y. In the specimen 22E, it is observed that the studs of the L-shaped damper extended and elongated at positive loads and folded down and shortened in negative loads starting from the first load cycles. Micro cracks were detected at the tip of the damper studs at 0.03 radians rotation. Due to single skewedness of L-shaped dampers, the stability of the compression side of the damper could be lost in a short time irrespective of the load direction and thus, the double-skewed damper 15E which has studs skewed in two opposite directions was designed and produced. Since the cracks concentrated at the tips of the damper studs for the rest of the dampers, the thickness of the damper studs was increased in order to prevent damage at the ends due to stress concentration at the sharp stud corners. The double-skewed L-shaped damper achieved similar load carrying capacities for positive and negative load cycles. Micro cracks were detected at the end of the damper studs at 0.02 radians rotation. The specimen 12D carried 3% less moment than the beam's theoretical plastic moment capacity and the theoretical elastic limit was not exceed. Therefore, no damage on the beam was observed. Although the specimen 15D carried 11% more moment than the theoretical plastic moment capacity of the beam, no damage was observed on the beam owing to the stiffeners welded on the potential plastic hinge location. It was determined that the specimens 15Y carried 2% more, 22E carried 4% less and 15E carried %5 more moment than the beam's plastic moment capacity.

As expected, the panel zone reinforced with stiffeners remained within the elastic range and exhibited a strong panel zone behavior. Figure 9-14 shows that 0.03 radians plastic rotation was exceed at all joints.

The hysteresis curves of the load and the displacement values measured at the free-end of the beam for every test specimen are provided in Figure 16.

Buckling of the reference specimen

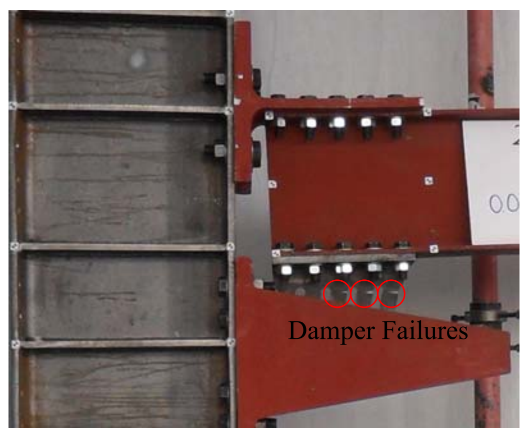

Failure of the damper studs of specimen 12D

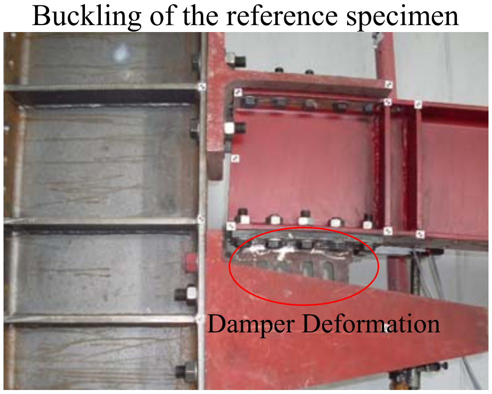

Damper deformation of specimen 15D

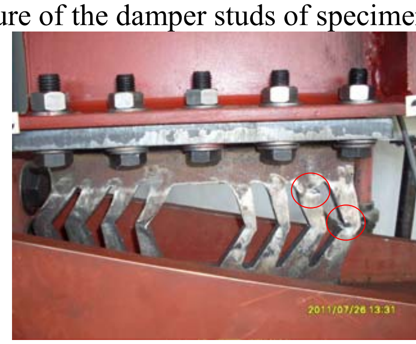

Failure of the studs of specimen 15E

Failure of the damper studs of specimen 15Y

Failure of the damper studs of specimen 22E

Figure 15. Damage Photos from the Tests

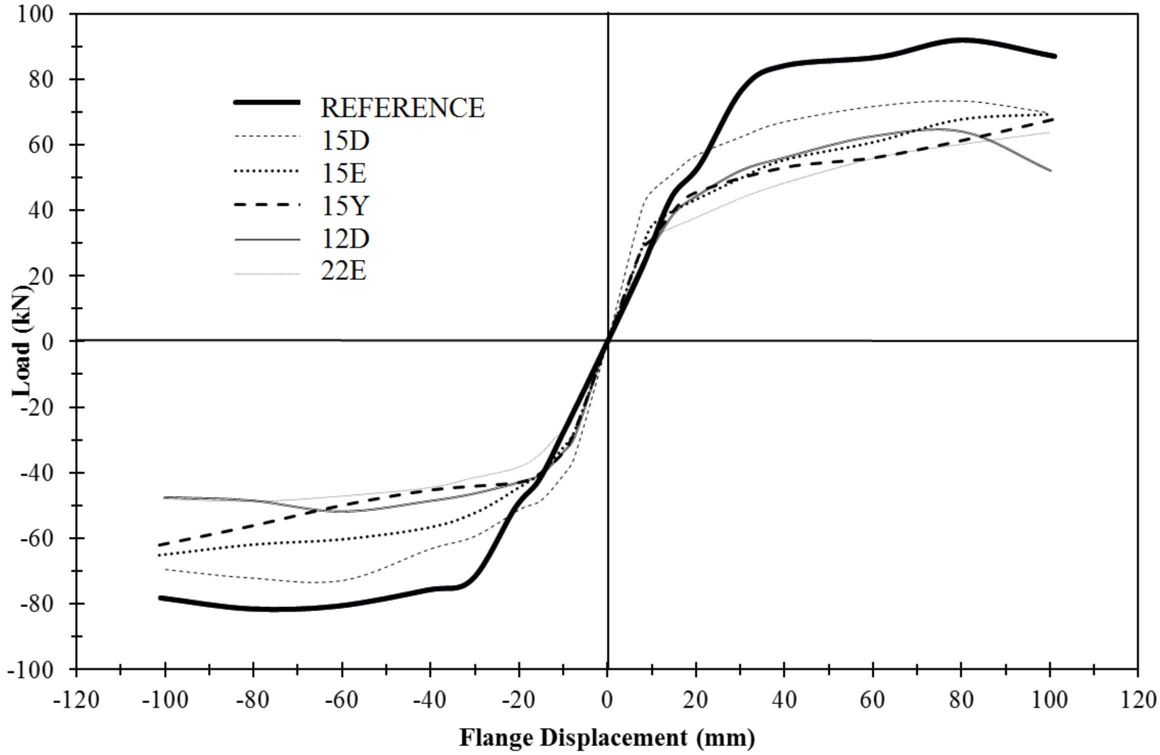

Figure 16. Load-displacement Hysteresis Curve of all Specimens

The plastic hinge formation caused the stiffness of the specimens to reduce during cyclic loading. The slope of the load-displacement curve at each load cycle is determined and the stiffness reduction graph was generated (Figure 17).

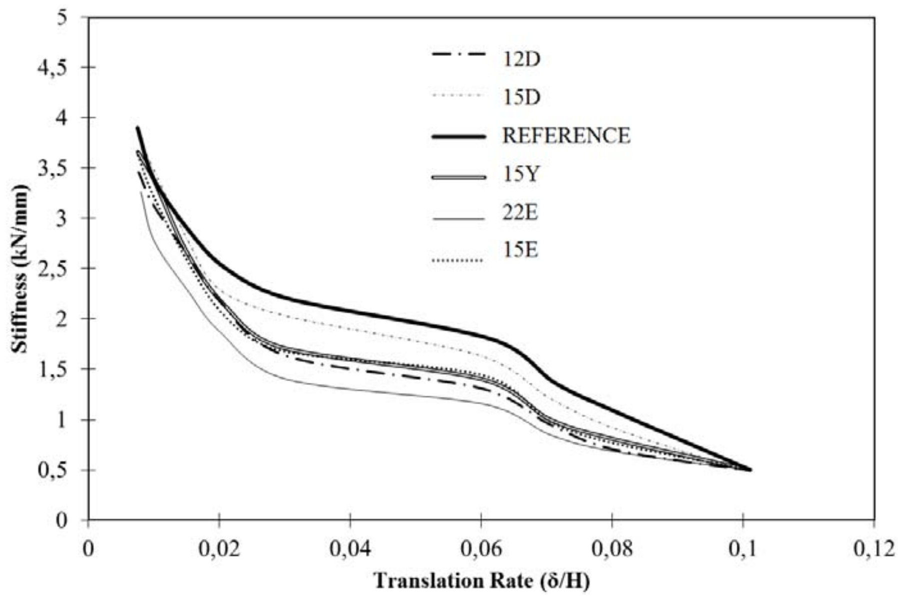

Figure 17. Stiffness Reduction Graph

Frame systems subjected to lateral cyclic loads consume a part of the produced energy by deformations. Amount of the consumed energy is quite important particularly in the case of dynamic loads such as earthquakes. Energy is equal to the work done, while the work is equal to force multiplied by distance. Therefore, the energy consumed by the test specimen is equal to the area under the load-displacement curve for each cycle. In this study, as seen in Figure 18, test specimens 12D, 15D, 15E, 15Y consumed 9%, 4%, 10%, and 13% less energy than the reference specimen, respectively. The specimen 22E, however, exhibited quite a ductile behavior and consumed 8% more energy than the reference specimen (Figure 18).

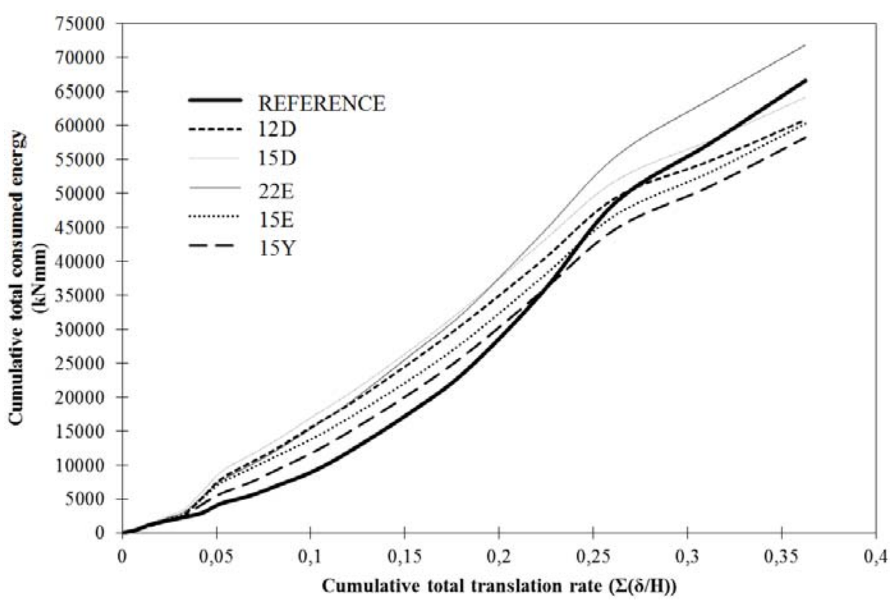

Figure 18. The graph of Total Consumed Energy

Considering the stiffness and the consumed energy, the specimen 15D with 15 mm thick damper performed best among the tested dampers. It has the highest stiffness and carried 11% more moment than the theoretical plastic moment of the beam. Although specimen 22E has higher energy consumption than 15D, its stiffness was the lowest of all dampers.

7. ANALYTICAL STUDY

In this section, the nonlinear model of the beam-column joint of a steel frame subjected to cyclic loading was created by using finite element method (FEM) so that the results of the experiments and of the numerical analysis could be compared. Hysteretic behavior of the considered beam-column joint was obtained by determining the stresses and deformations at various stages of the loading. For the nonlinear analyses, the required material models for each material type were obtained. Each material model was numbered and the numbers were assigned to the elements. The stress-strain curves obtained from the tensile tests of St-44 and St-37 type steel specimens were used for the column, beam, gusset and top T members, and for dampers, respectively.

3D model geometry was meshed using Solid 187 element type available in ANSYS library. Solid 187 is a 3D, 10-node tetrahedral solid element with mid-nodes. It has quadratic displacement behavior and is widely used in modeling irregular meshes. It has three translational degrees of freedom at each node in x, y and z directions (Figure 19). The average element size near beam-column connection was 12 mm. Coarser meshing was applied away from the joint where the average element size became 20 mm. The contacting surfaces between steel plates were assumed to be perfectly bonded. In order to see the stress concentrations around the bolt holes, they were included in the model. However, the bolts were not modeled. The column was fixed at top and bottom surfaces through 70 mm distance from the free edges. The load was applied at the centerline of the beam section at 2 m away from the face of the column connection plate.

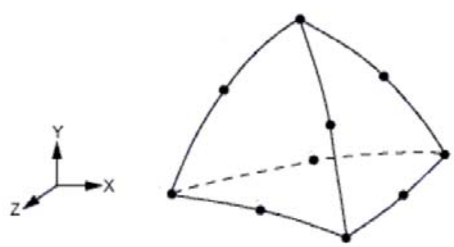

Figure 19. General Geometry and Nodes of Solid 187 Element

The steel material was assumed to have the stress-strain relationship presented in Figure 20. This stress-strain diagram was used in the definition of “Multilinear Kinematic Hardening” material model in order to simulate the behavior under cyclic loading given in Figure 21. This hardening model considers the Bauschinger effect so that the yield surface remains constant in size and translates in the direction of yielding. In Figure 20, the initial slope is equal to the first yielding stress divided by the corresponding strain and is defined as the modulus of elasticity of steel. The Poisson’s ratio was assumed to be 0.3, as usual.

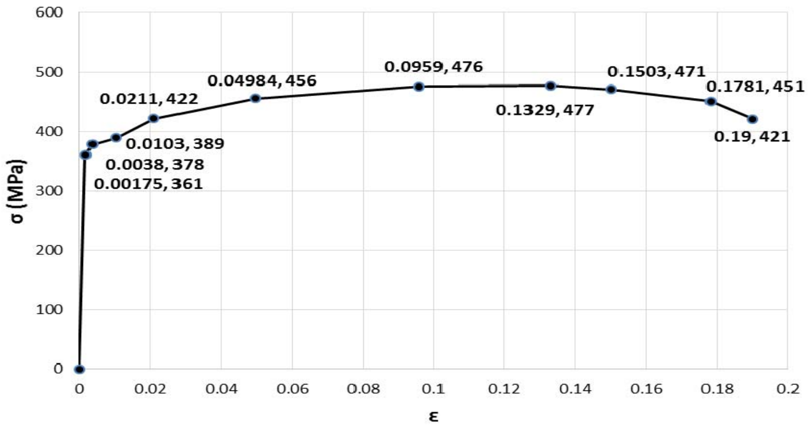

Figure 20. Stress-strain Model of the Steel Material

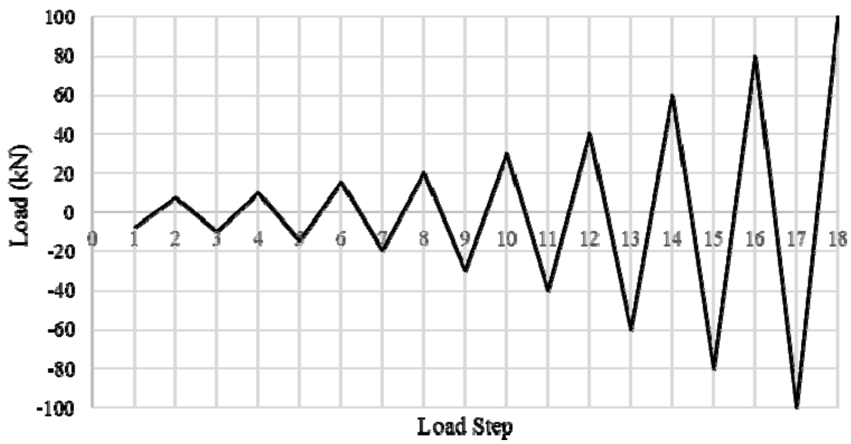

Figure 21. Applied Cyclic Loading Scheme

During the FE analysis, material and geometry nonlinearities were both considered. Iterative analysis was carried out using Newton Raphson method. The cyclic load history was applied with sufficiently small increments to obtain a convergent nonlinear solution. A cyclic loading text input file was prepared to be read from the File pull-down menu while Solution menu tree was kept active. The file has twice as many lines as the number of loadings. One line contains a displacement command with the loaded node number, loading direction and the amount of load and the following line contains the solve command; such as:

D,63303,UX,-7.5
SOLVE
D,63303,UX,7.5
SOLVE
…

In order to draw the force-displacement history plot within ANSYS Time History post-processor, a macro file was generated. After defining the array of the fixed node numbers for each load step increment, the reaction forces at fixed nodes in the loading direction were summed up and combined with the calculated displacement at the location and direction of loading to obtain the load-displacement plot.

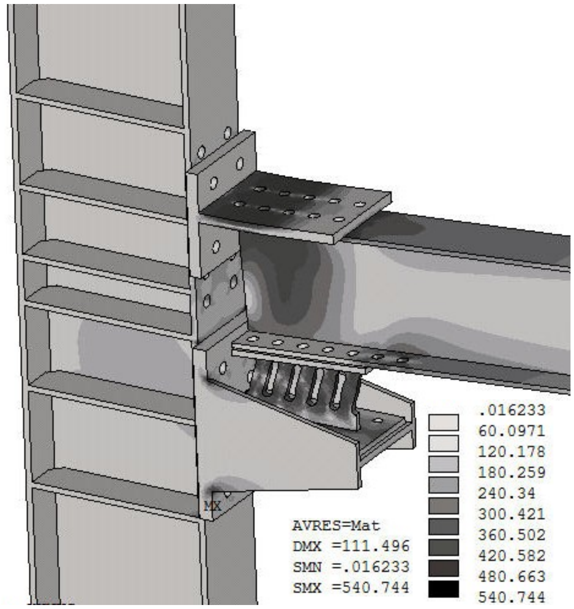

Specimen 12D

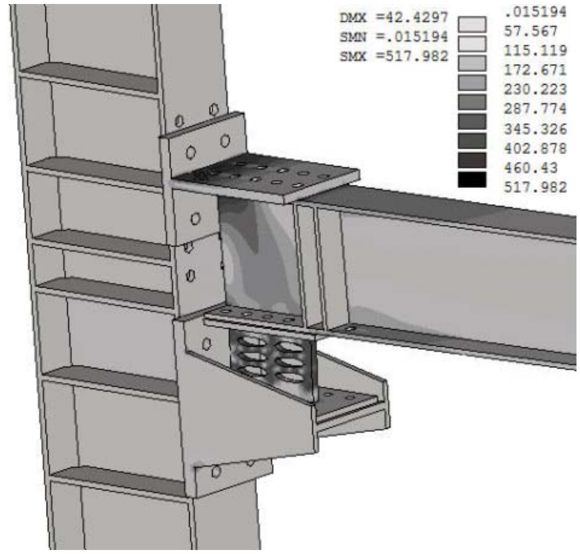

Specimen 15Y

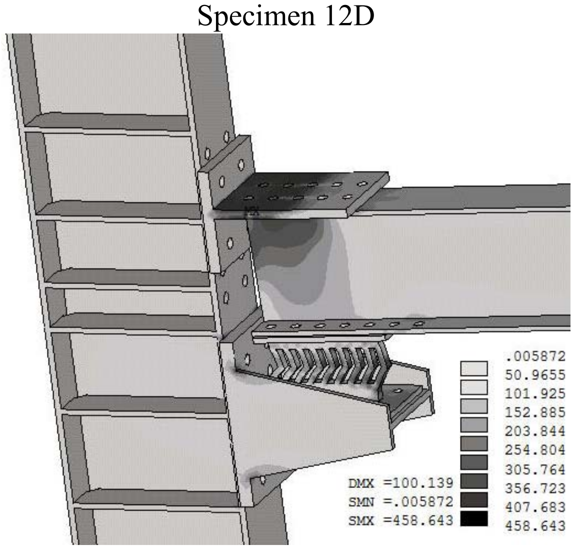

Specimen 22E

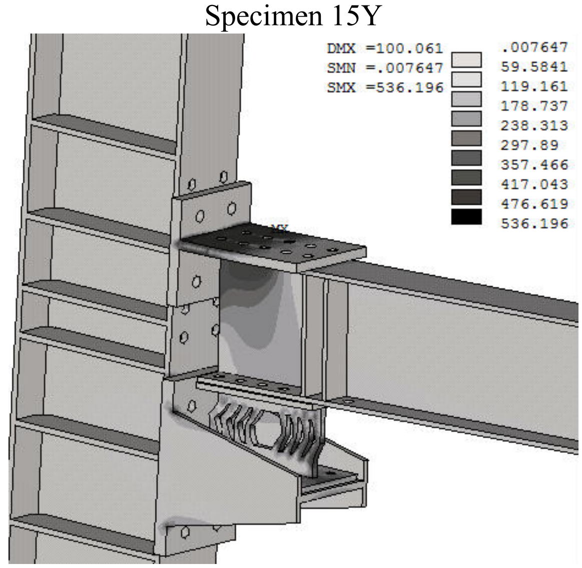

Specimen 15E

Figure 22. Von Misses Stress Contours of Specimens

Von misses stress contours of the specimens are given in Figure 22 and comparison of load-displacement graphs of the specimens are given in Figures 23-27.

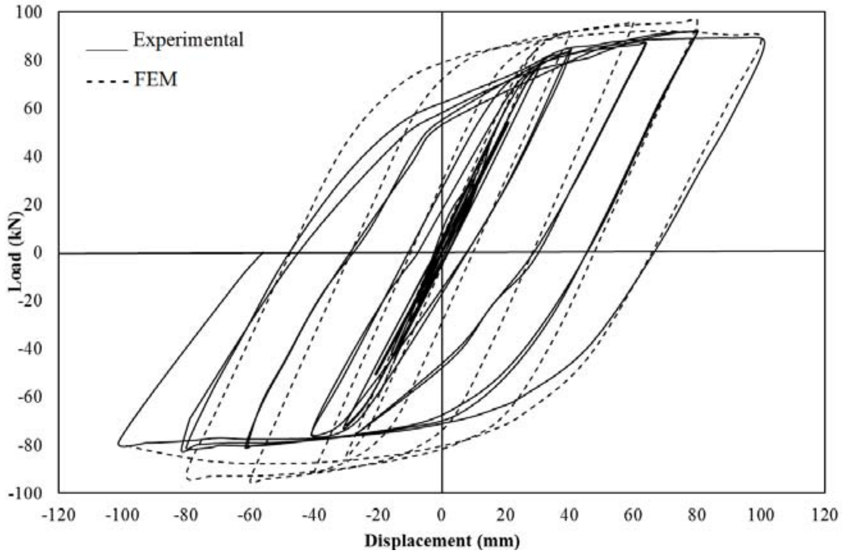

Figure 23. Load-displacement Curve Comparison of Reference Specimen

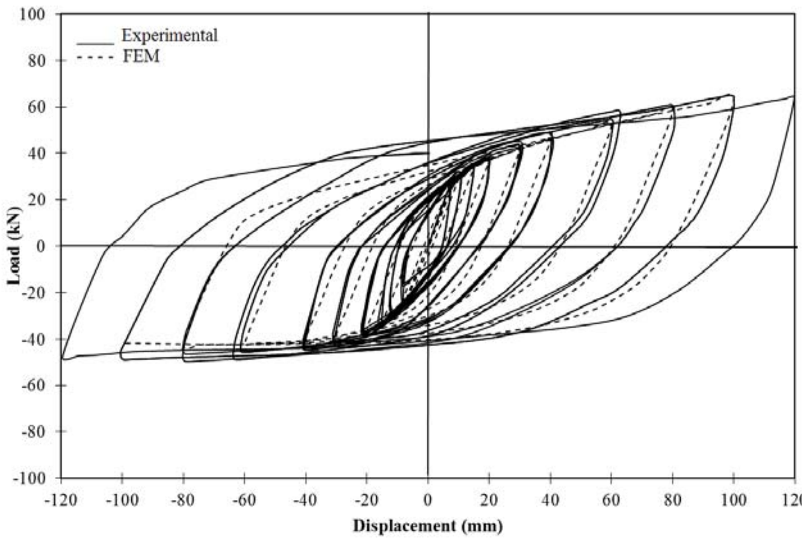

Figure 24. Load-displacement Curve Comparison of Specimen 22E

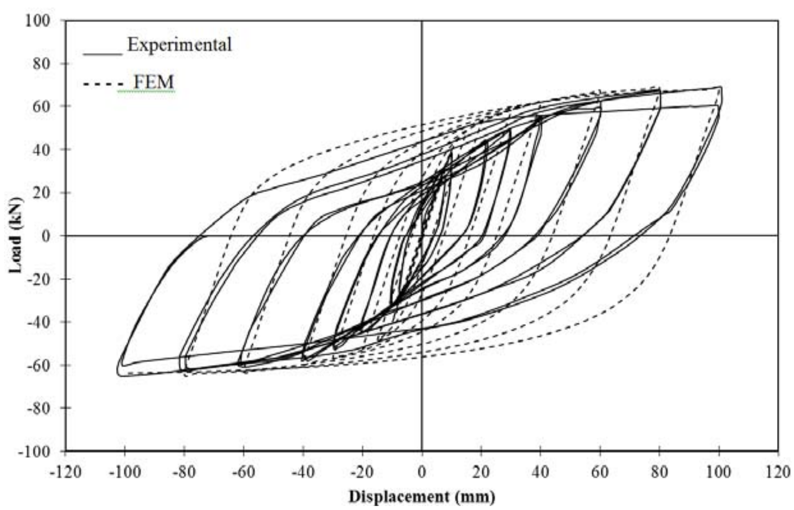

Figure 25. Load-displacement Curve Comparison of Specimen 15 E

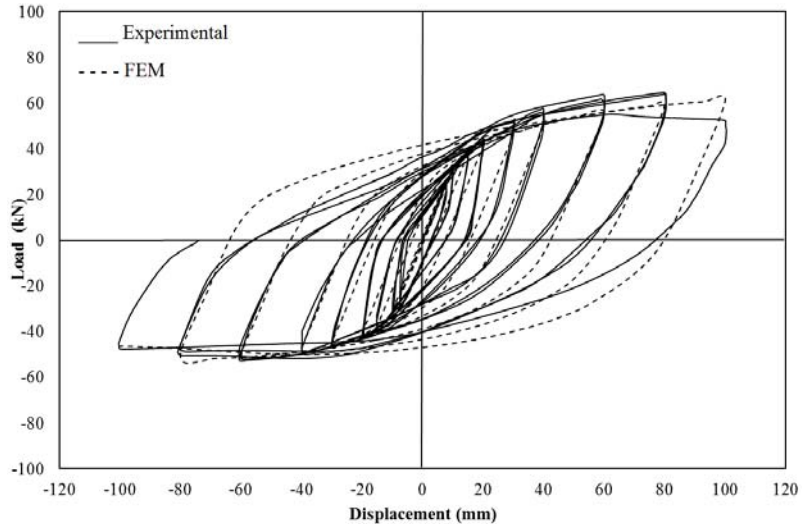

Figure 26. Load-displacement Curve Comparison of Specimen 12D

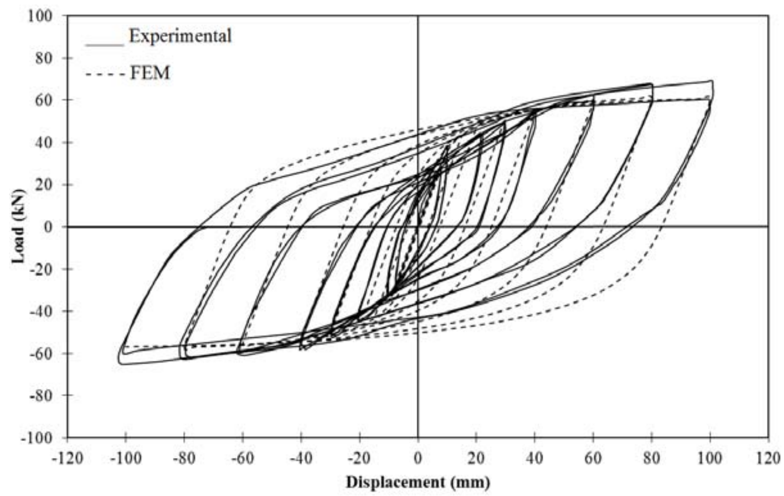

Figure 27. Load-displacement Curve Comparison of Specimen 15 Y

8. RESULTS

The use of slit dampers at beam-column joints of steel frames was investigated analytically by ANSYS Finite Element Software package. It was observed that the experimental and analytical cyclic loading vs. displacement curves were quite close to each other for each test specimen. For the reference specimen, the load values obtained from FEM analysis were found to be higher than the experimental ones. This might be attributed to the reduction in the strength because of the possible micro cracks occurred during the welding of the end plate and the beam. FEM analysis of the specimen 22E resulted in slightly lower load values in the compressive load cycles compared to its experimental counterparts. The approximate values of the peak loads and load cycles indicate that specimens were modeled successfully.

The purpose of this study was damping the energy by the yielding of dampers in order to prevent any possible beam damage at the joint of a steel beam-column under cyclic loads. The applied load that caused yielding of the IPE 270 beam was calculated approximately as 64 kN. In the experimental study, specimen 12D carried a load as much as the calculated theoretical load. In addition, since the damper yielded by damping the energy before any yielding occurred on the beam of the specimen 12D, no permanent damage was observed either on the beam or the column. The maximum load that can be carried by the specimen N12 from FEM analysis is 5% lower than the experimentally determined load. Damper thickness of the specimen 15D was increased from 12 mm to 15 mm unlike in the specimen 12D. At the same time, in order to prevent a possible damage to the beam, it is reinforced with two stiffeners at the damper ends. The purpose was to increase the load carrying capacity of the joint by preventing a permanent damage to the beam even above the theoretical yield load. The experimental studies showed that a load 15% more than the beam's yield load was carried by the specimen 15D without any damage. It was observed that the highest load value obtained from FEM analysis was 4% less than the experimental one. Specimen 15Y carried 2% more load, as well, than the beam's yield load. In the specimen, the damage was concentrated on the dampers and the beam reinforced by stiffeners had no damage. Exhibiting quite a ductile behavior, specimen 22E carried a load up to the beam's yield limit. FEM model of this specimen displayed the reduction in the load-carrying capacity in the unloading region. Reinforced with stiffeners and attached an L-shaped slit damper skewed in both directions, specimen 15E carried 10% more load than the beam's yield limit and the FEM model was able to approximately simulate this behavior. In the meantime, although the ultimate load carried by the reference specimen was larger than the load carried by all damper added specimens, it was observed that energy consumption rate was not that high. As a matter of fact, specimen 22E consumed 8% more energy. The maximum load carried by the end plated reference specimen was 30%, 19%, 23%, and 26% higher than that of the specimens 12D, 15D, 15E and 15Y, respectively. However, the energy consumed by reference specimen was 9%, 4%, 10% and 13% higher than that of the specimens 12D, 15D, 15E and 15Y, respectively. The reason for this was that the damper yielded before the beam in the damper attached specimens and it absorbed the energy in a ductile manner during collapse.

Table 3. Comparison of Experimental and FEM Results

Specimens	Maximum experimental load carried at the beam end (kN)	Maximum load obtained from FEM (kN)	Experimental to FEM ratio
Reference	91	96	0,95
15D	73	70	1,04
12D	64	61	1,05
15E	70	68	1,03
15Y	68	61	1,11
22E	64	63	1,02

9. CONCLUSIONS

In this paper, experimental and analytical studies were conducted on the behavior of steel slit dampers which can be replaced in an easy, fast and economical way in order to allow putting a steel framed structure back into service immediately after a major earthquake by preventing the damage to the structural system. Therefore slit dampers were considered for this study and the damper geometries were decided based on some preliminary tests. For this purpose, in addition to one conventional end plated joint (reference system), five damper-attached joints: one with 12 mm and the other with 15 mm thick slit dampers, one with 15 mm thick round hole damper, one with 22 mm thick L shaped (single skewed) and the other with 15 mm thick L shaped (double-skewed) damper; were constructed with full scale and experimentally tested in order to evaluate their performance. The 3D Finite Element Model of the tested specimens was created and the nonlinear analyses were performed using ANSYS software package.

The conclusions drawn from the experimental and analytical research are noted below:

1. The proposed damper systems exhibited a stable hysteretic behavior under large story drift. First cycle stiffness rates of two damper attached systems are larger than that of the end plate connected joint and thus, the proposed systems are quite rigid.
2. Proposed damper systems are designed considering the theoretical yield strength of the beam thus enabling the concentration of plastic deformations when the beam and column are within the elastic range at the joints and preventing the damage to the beam and column.
3. FEM analyses which are based on the realistic and nonlinear modeling of the materials used in the experiments produced very similar results to the experimental ones. The cyclic behavior of the test specimens was modeled reasonably and with sufficient approximation.
4. Despite the stable behavior and high plastic deformation capacity of conventional end plate connected joints, the local buckling of the beam after a possible earthquake indicates that the repair and strengthening of the beam is ineffective and unreasonable.
5. It is possible to carry loads and moments up to a certain level of the beam capacity by attaching dampers to a beam-column joint of a steel frame without having any damage on the beam or column. When the loads and moments reach critical levels, the dampers exhibit their expected behavior by first yielding and then reaching their limit states with no damage to the beam and column.
6. The damper produced with L shaped slits consumes a high amount of energy, however, it has a low load carrying capacity in one direction of a cyclic load.
7. It is observed that the geometry of the dampers changed not only the load bearing capacity but also the behavior such as ductility and stiffness.
8. In order to fully grasp the behavior of the proposed damper systems, further research can be performed by first developing different joint and damper types and their FEM models, and then testing them experimentally.

ACKNOWLEDGMENTS

This paper was supported by Scientific Research Projects Office of Selcuk University with Project No. 10101008 and The Scientific and Technological Research Council of Turkey (TUBITAK) with Project No. 110M022.

REFERENCES

[1] Oh, S.-H., Kim, Y.-J. and Ryu, H.-S., "Seismic Performance of Steel Structures with Slit Dampers", Engineering Structures, 2009, Vol. 31, No. 9, pp. 1997-2008.

[2] Bergman, D.M. and Goel, S.C., "Evaluation of Cyclic Testing of Steel-plate Devices for Added Damping and Stiffness", 1987, Department of Civil Engineering, University of Michigan.

[3] Tsai, K.-C., et al., "Design of Steel Triangular Plate Energy Absorbers for Seismic-resistant Construction", Earthquake Spectra, 1993, Vol. 9, No. 3, pp. 505-528.

[4] Kobori, T., et al., "Development and Application of Hysteresis Steel Dampers", Proceedings of the 10th World Conference on Earthquake Engineering. 1992.

[5] Sabelli, R., Mahin, S. and Chang, C., "Seismic Demands on Steel Braced Frame Buildings with Buckling-restrained Braces", Engineering Structures, 2003, Vol. 25, No. 5, pp. 655-666.

[6] Clark, P., et al. "Design Procedures for Buildings Incorporating Hysteretic Damping Devices", Proceedings 68th annual convention. 1999.

[7] Lee, M.H., et al., "Ultimate Energy Absorption Capacity of Steel Plate Slit Dampers Subjected to Shear Force", International Journal of Steel Structures, 2002, Vol. 2, No. 2, pp. 71-79.
[8] Chan, R.W. and Albermani, F., "Experimental Study of Steel Slit Damper for Passive Energy Dissipation", Engineering Structures, 2008, Vol. 30, No. 4, pp. 1058-1066.
[9] Köken, A. and Köroğlu, M.A., "An Experimental Study on Energy Absorption Capacity of steel dampers subjected to shear force" Int. J. Arts Sci., 2011, Vol. 4, No. 2, pp. 25-32.
[10] Köken, A., and Köroğlu, M. A., "Waste Rubber Damper using on Steel Beam to Column Connection," Int. J. Arts Sci., 2012, Vol. 5, No. 4, pp. 217-222.
[11] Koken, A. and Köroğlu, M.A., "Steel Plate Slit Damper using on Steel Frames" e-J. New World Sci. Acad., 2011, Vol. 6, No. 4.
[12] Köken, A. and Köroğlu, M.A., "Experimental Study on Beam-to-Column Connections of Steel Frame Structures with Steel Slit Dampers," Journal of Performance of Constructed Facilities", 2013, Vol. 29, No. 2, pp. 04014066.
[13] Köroğlu, M., "Seismic Damper using on Beam to Column Connections of Steel Frames", Doctor of Thesis, Selcuk University, Institute of Graduate and Applied Sciences, Konya, Turkey, 2012.
[14] Saffari, H., Hedayat, A. and Nejad, M.P., "Post-Northridge Connections with Slit Dampers to Enhance Strength and Ductility", Journal of Constructional Steel Research, 2013, Vol. 80, pp. 138-152.
[15] Pachoumis, D., et al., "Cyclic Performance of Steel Moment-resisting Connections with Reduced Beam Sections-experimental Analysis and Finite Element Model Simulation", Engineering Structures, 2010, Vol. 32, No. 9, pp. 2683-2692.
[16] Committee, S.J.V.G.D., et al., "Recommended Seismic Evaluation and Upgrade Criteria for Existing Welded Steel Moment-frame Buildings", 2000: FEMA.